JLB

Article

The synaptic recruitment of lipid rafts is dependent on CD19-PI3K module and cytoskeleton remodeling molecules

Liling Xu,[*,†,‡,1] Arturs Auzins,*[*,†,1] Xiaolin Sun,[§,1] Yinsheng Xu,*[*,†] Fiona Harnischfeger,*[*] Yun Lu,[¶] Zhanguo Li,[§] Ying-Hua Chen,*[*,2] Wenjie Zheng,[‡] and Wanli Liu*[*,†,2]

*MOE Key Laboratory of Protein Science, School of Life Sciences, and [¶]State Key Joint Laboratory of Environment Simulation and Pollution Control, School of Environment, Tsinghua University, Beijing, China; [†]Collaborative Innovation Center for Infectious Diseases, Hangzhou, China; [§]Department of Rheumatology and Immunology, Clinical Immunology Center, Peking University People's Hospital, Beijing, China; [‡]Department of Rheumatology and Clinical Immunology, Peking Union Medical College Hospital, Peking Union Medical College and Chinese Academy of Medical Sciences, Beijing, China; and Key Laboratory of Rheumatology and Clinical Immunology, Ministry of Education, Beijing, China

RECEIVED JUNE 6, 2014; REVISED APRIL 14, 2015; ACCEPTED APRIL 15, 2015. DOI: 10.1189/jlb.2A0614-287RR

ABSTRACT

Sphingolipid- and cholesterol-rich lipid raft microdomains are important in the initiation of BCR signaling. Although it is known that lipid rafts promote the coclustering of BCR and Lyn kinase microclusters within the B cell IS, the molecular mechanism of the recruitment of lipid rafts into the B cell IS is not understood completely. Here, we report that the synaptic recruitment of lipid rafts is dependent on the cytoskeleton-remodeling proteins, RhoA and Vav. Such an event is also efficiently regulated by motor proteins, myosin IIA and dynein. Further evidence suggests the synaptic recruitment of lipid rafts is, by principle, an event triggered by BCR signaling molecules and second messenger molecules. BCR-activating coreceptor CD19 potently enhances such an event depending on its cytoplasmic Tyr421 and Tyr482 residues. The enhancing function of the CD19-PI3K module in synaptic recruitment of lipid rafts is also confirmed in human peripheral blood B cells. Thus, these results improve our understanding of the molecular mechanism of the recruitment of lipid raft microdomains in B cell IS. *J. Leukoc. Biol.* 98: 223–234; 2015.

Introduction

The activation of B cells is initiated by the immune recognition of antigens by the clonally expressed BCRs [1–3]. The signaling cascades of B cell activation have been investigated extensively in the past decade by biochemical studies [2, 4], which also show that lipid rafts, which are detergent-resistant, sphingolipid, and cholesterol-rich membrane fractions, play an important role in the initiation of B cell activation [5–8]. Lipid rafts represent >40% of the plasma membrane lipids of immune cells [9]. Lipid rafts have a central feature of segregating membrane proteins, thereby providing a mechanism to compartmentalize BCR signaling proteins [7, 8]. Indeed, it is known that multivalent antigen binding to BCRs induces the translocation of clustered BCRs to the lipid rafts, where BCRs could encounter Lyn kinase and get phosphorylated, and thus, BCR signaling gets initiated. It is noteworthy that the strength of the initiated BCR signaling is positively correlated with the stability of the association between clustered BCR and lipid rafts [6, 10]. Moreover, such association is under strict regulation by BCR inhibitory coreceptors FcγRIIB and activating coreceptor CD19. BCR and FcγRIIB coligation destabilizes the association of BCR and lipid rafts, which in turn, potently inhibits the initiation of B cell activation [11]. In contrast, the coligation of BCR and CD19 increases the amount of BCRs that are translocated into lipid rafts and prolongs their subsequent residency in the lipid rafts, which vigorously enhances the initiation of B cell activation [12, 13].

The recent advances in high-resolution live cell and molecule imaging technologies provided another layer of dynamic, complicated, and yet an ordered set of molecular events during the initiation of B cell activation that follows within seconds after antigen recognition by the BCRs [14, 15]. Different from the biochemical studies, these optical-based imaging studies generally use membrane-bound antigens to activate B cells, which is the major format of the antigens that B cells would likely encounter in vivo [16–19]. Fleire et al. [20] first showed the molecular events that follow the encounter of B cells with antigen containing fluid PLBs serving as a surrogate for APCs. They

Abbreviations: CFP = cyan fluorescent protein, CTB = cholera toxin B subunit, DAG = diacylglycerol, DGK = diacylglycerol kinase, FP = fluorescent protein, GEF = guanine nucleotide exchange factor, H12-D-domain = polyhistidine (H12) tag fused to the N terminus of the D domain of staphylococcal protein A, HPI-4 = hedgehog pathway inhibitor, IRM = interference reflection microscope, IS = immunological synapse, MFI = mean fluorescence intensity,

(*continued on next page*)

The online version of this paper, found at www.jleukbio.org, *includes supplemental information.*

1. These authors contributed equally to this work.
2. Correspondence: School of Life Sciences, Tsinghua University, Beijing, China, 100084. E-mail: liuwanli@biomed.tsinghua.edu.cn (W.L.); chenyh@tsinghua.edu.cn (Y-H.C.); Department of Rheumatology and Clinical Immunology, Peking Union Medical College Hospital Beijing, China, 100730. E-mail: wenjzheng@gmail.com (W.Z.)

showed that B cells first dramatically spread over the antigen containing PLBs concomitant with the formation of BCR microclusters in the peripheral lamellipodias of the cell. Following maximal spreading, B cells subsequently contract to form an ordered IS [20]. With the use of TIRFM-based, high-resolution imaging, our previous study suggests that the recognition of BCR and antigen drives the growth feature of BCR microclusters [21]. The following study determines that the growth of BCR microclusters is an important step accounting for the formation of B cell IS [14, 21–24]. More importantly, Sohn et al. [25] showed that BCR cross-linking induced the transient interaction of BCR microclusters and lipid rafts, and lipid rafts function as a hub to promote the coclustering of BCR and Lyn kinase microclusters within the B cell IS [26]. With the consideration of the importance of both B cell IS and lipid rafts in the initiation of B cell activation, it is of great interest to identify the molecular machineries supporting the efficient recruitment of lipid rafts into B cell IS upon engaging BCRs by membrane-bound antigens. In this report, we address this question by use of TIRFM-supported, high-resolution live cell imaging techniques in combination with mutagenesis and pharmaceutical inhibitors.

MATERIALS AND METHODS

Cells, antigens, and antibodies

A20II1.6, CH27, and J558L B cell lines were gifts from Dr. Susan K. Pierce [National Institute of Allergy and Infectious Diseases, National Institutes of Health (NIH), Bethesda, MD, USA] and all of them were purchased originally from American Type Culture Collection (Manassas, VA, USA). Biotin-conjugated goat $F(ab')_2$ anti-mouse IgM + IgG (H+L), biotin-conjugated goat $F(ab')_2$ anti-human IgA + IgG + IgM (H+L), rabbit Fab anti-mouse IgM specific for Fc5μ, and rabbit Fab anti-mouse IgG specific for the Fc portion were purchased from Jackson ImmunoResearch Laboratories (West Grove, PA, USA). Biotin-conjugated anti-mouse CD32/CD16 (clone no. 2.4G2), biotin-conjugated anti-mouse CD19 (clone no. 1D3), and biotin-conjugated hamster anti-mouse/rat CD81 (clone no. Eat2) were purchased from Becton Dickinson (Franklin Lakes, NJ, USA). Biotin-conjugated anti-mouse CD21/CD35 (CR2/CR1; clone no. eBio8D9) and anti-mouse CD19 purified (MB19-1) were purchased from eBioscience (San Diego, CA, USA). Alexa Fluor 568-conjugated goat Fab anti-human IgG specific for the Fc portion and secondary antibody Alexa Fluor 568-conjugated $F(ab')_2$ goat antibodies specific for rabbit IgG were acquired from Invitrogen (Carlsbad, CA, USA). Phospho-Zap-70 (Tyr319)/Syk (Tyr352)-, phospho-CD19 (Tyr531)-, and phospho-PI3K p85 (Tyr458)/p55 (Tyr199)-specific antibodies were purchased from Cell Signaling Technology (Danvers, MA, USA). Goat Fab anti-mouse CD19 (clone no. 1D3) and mouse Fab anti-human CD19 (clone no. HIB19) were made by use of a Fab micropreparation kit following a protocol in our published studies [21, 22, 27–29]. Alexa Fluor 488-conjugated CTB and Alexa Fluor 647-conjugated CTB were purchased from Life Technologies (Carlsbad, CA, USA). Conjugations of antibodies with Alexa Fluor (Alexa Fluor 405, 488, 568, or 568) were carried out by use of Alexa Fluor mAb labeling kits (Molecular Probes, Eugene, OR, USA), following the manufacturer's protocols, whereas biotinylated antibodies or NP32-BSA (Biosearch Technologies, Petaluma, CA, USA) were carried out following the manufacturer's protocols of EZ-Link sulfo-NHS-LC-biotin (Thermo Fisher Scientific, Waltham, MA, USA).

(*continued from previous page*)

NP = 4-hydroxy-3-nitrophenyl acetyl, PIP_2 = phosphatidylinositol 4,5-bisphosphate, PLB = planar lipid bilayer, PLC = phospholipase C, ROI = region of interest , TFI = total fluorescence intensity, TIRFM = total internal reflection fluorescent microscopy, WT = wild-type, YFP = yellow fluorescent protein

Pretreatment of inhibitors

Cells were pretreated with the inhibitors under different conditions following protocols in published studies or the manufacturer's instructions. For wortmannin (Calbiochem, San Diego, CA, USA) and LY294002 (Life Technologies), the working concentration was 100 nM [30] and 20 μM [31], respectively, and the cells were incubated for 1 h at 37°C. Likewise, cells were incubated for 30 min at 37°C for these following inhibitors at the indicated working concentration following the published protocols: 10 mM methyl-β-cyclodextrin (Sigma-Aldrich, St. Louis, MO, USA) [3], 10 μM paclitaxel [32], 50 μM blebbistatin [33], 5 μM DGK inhibitor II [34], and 40 μM BAPTA/AM [35]. Cytochalasin D was used at 0.2 μM, cells were incubated for 10 min at 37°C [36], jasplakinolide was 1 μM, and cells were incubated for 45 min at 37°C [21]. To disrupt the tubulin-cytoskeleton filaments efficiently, B cells were pretreated with 2 μM nocodazole for 1 h at 4°C, followed with another 0.5 h at 37°C [21]. The working concentration of HPI-4 was 30 μM, and cells were incubated overnight at 37°C [37]. 6-Thio-GTP (Jena Bioscience, Jena, Germany) was used at a 50 μM concentration, and cells were incubated for 2 d at 37°C [38]. ML-7 (Calbiochem) was used at 10 μM concentration, and cells were incubated for 20 min at room temperature [39]. For RhoA activator and RhoA inhibitor (Cytoskeleton, Denver, CO, USA), the working concentration was 2 and 5 μM, respectively, following the manufacturer's instructions. The dosage and procedure of DMSO treatment were exactly matched to each inhibitor to serve as an intragroup negative control. After the inhibitor treatment at their respective described conditions above, the cells were washed 3 times with PBS and were ready for further processing.

Plasmid constructs and transfections

The pEYFP-N1 and pECFP-N1 were purchased from Clontech (Mountain View, CA, USA). To reduce the dimerization of YFP, the YFP gene was modified by use of a QuikChange II XL site-directed mutagenesis kit (Stratagene, La Jolla, CA, USA), as suggested in a published study [40]. The sequence of Lyn-m16 was cloned into pEYFP-N1, pECFP-N1, and pEYFP-N1, in which YFP was swapped for mCherry. For the expression of vectors, cells from A20II1.6 and CH27 cell lines were transfected by electroporation, selected for growth in 0.5 or 1 mg/ml G418, and sorted by Lyn-m16-YFP or Lyn-m16-CFP expression by use of flow cytometry. Mouse CD19 was amplified with the primers 5′- ATGCCATCTCCTCTCCCTGTC -3′ and 5′-TTACGTGGTTCCCCAAGTCCCC -3′ and subcloned in pEYFP-N1 after adding the stop code in which YFP was not expressed. The mutagenesis was done by the Gibson assembly method, as described previously [41].

Isolation of human PBMCs

This study was approved by Ethics Committee of Peking Union Medical College Hospital, and all healthy volunteers provided the informed consent documents. Peripheral blood (4 ml) was acquired from each of 6 healthy volunteers. The isolation of PBMCs from these samples was done by following the manufacturer's protocols of Ficoll-Paque PLUS density separation and frozen until imaging experiments took place.

Preparation of antigen-containing PLBs

Biotin-containing PLBs were prepared following our published protocol [21, 22, 29, 42]. Biotinylated anti-IgG or anti-IgM antibodies served as surrogate antigens, biotin-conjugated NP32-BSA, and biotinylated anti-FcγRIIB, or biotinylated anti-CD19 antibodies were attached to biotin-containing PLBs through streptavidin. In brief, the coverslips were incubated with 0.1 mM biotin liposomes in PBS for 20 min. After washing with 10 ml PBS, the PLB was incubated with 40 nM streptavidin for 15 min, and excessive streptavidin was washed away with 10 ml PBS. The streptavidin-containing PLBs then were incubated with 10 nM biotinylated goat $F(ab')_2$ anti-mouse IgM + IgG (H+L) or biotinylated NP32-BSA to cross-link BCR alone for 15 min. To coligate the BCR and FcγRIIB or CD19, the streptavidin-containing PLBs were incubated with an additional 20 nM biotinylated IgG anti-mouse FcγRII/FcγRIII or biotinylated IgG anti-mouse CD19, whereas the control group was incubated with 20 nM biotinylated nonspecific mouse IgG. The excessive antigen was

washed away by 10 ml PBS, and PLBs were blocked with 5% BSA in PBS for 30 min at 37°C and then washed thoroughly for further use.

PLBs for human primary B cells stimulation were prepared by use of an antibody against BCR and an antibody against CD19, which tethered to a nickel PLB through an H12-D-domain, as described previously [43]. In brief, the coverslips were incubated with 0.1 mM nickel nitrilotriacetic acid-containing liposomes in PBS for 20 min. After washing with 10 ml PBS, the PLBs were incubated with a 50 nM H12-D-domain for 20 min at room temperature. After washing thoroughly, PLBs were incubated with a 15 nM goat IgG anti-human λ chain to cross-link BCR alone for 20 min following our published protocol [43]. To coligate the BCR and CD19, the PLBs were incubated with an additional 20 nM mouse IgG anti-human CD19, whereas the control group was incubated with 20 nM biotinylated, nonspecific mouse IgG. After washing again, PLBs was blocked with 5% BSA in PBS for 30 min at 37°C and washed thoroughly for later use.

TIRFM imaging and IRM imaging

A20II1.6 and CH27 cells were stained with Alexa Fluor 647-conjugated goat Fab anti-mouse IgG specific for the Fc portion or Alexa Fluor 647-conjugated goat Fab anti-mouse IgM specific for Fc5μ, respectively, and washed twice; then placed on PLBs, prepared as described in the figure legends for a different time duration at 37°C, 5% CO_2; and then fixed with 4% paraformaldehyde. Human primary B cells were stained with Alexa Fluor 647-conjugated goat Fab anti-human IgG specific for the Fc portion and Alexa Fluor 488-conjugated CTB, and then washed twice and placed on PLBs prepared as described for 5 or 10 min at 37°C, 5% CO_2, and then fixed with 4% paraformaldehyde. TIRF images were captured by use of an Olympus IX-81 microscope equipped with a TIRF port (Olympus, Center Valley, PA, USA), Andor iXon + DU-897D electron-multiplying charge-coupled device camera (Andor Technology, Concord, MA, USA), Olympus 100 × 1.49 NA objective TIRF lens, and a 488, 561, and 633 nm laser (Sapphire laser; Coherent, Santa Clara, CA, USA). Acquisition was controlled by Metamorph software (Molecular Devices, Sunnyvale, CA, USA) and with an exposure time of 100 ms for a 512 × 512 pixel image, unless specially indicated. IRM images were performed by use of the same Olympus IX-81 microscope with an Olympus 100 × 1.49 NA objective, as above, for TIRFM imaging experiments. Different from TIRFM imaging, a Pre-Aligned Intelli-Lamp system (X-Cite 120PC Q; Lumen Dynamics, Mississauga, Ontario, Canada) was used to provide the incident photons with a band-pass filter of 485/20 nm. In IRM imaging, a 483/32 nm band-pass filter was used. Images were analyzed by NIH ImageJ software, as our previous studies reported [21, 22, 29, 42]. In brief, images were subtracted for background and then marked with ROIs. The MFI values indicated the ratio of integrated fluorescence intensity of the ROIs to its total area of pixels. The TFI values indicated the integrated fluorescence intensity of the ROIs.

Images processing and mathematical and statistical analyses

The display range of a set of TIRFM images in each figure is the same to allow direct visional comparison of intensity unless indicated specifically. Student's *t*-test was performed for statistical comparisons. $P < 0.05$ was considered to indicate a significant difference.

RESULTS

Synaptic recruitment of lipid rafts is a cytoskeleton remodeling-dependent event

First, we assessed the effect of lipid rafts in the formation of BCR microclusters and B cell IS by pretreatment of A20II1.6 B cells with methyl-β-cyclodextrin to deplete cholesterol from the cell membrane, resulting in the disruption of the function of cholesterol- and sphingolipid-rich lipid rafts [3]. It is striking that methyl-β-cyclodextrin-pretreated B cells can hardly form an adhesion plan with the PLBs presenting the goat $F(ab')_2$ anti-mouse IgG antibodies as surrogate antigens (data not shown). These results are consistent with the earlier study showing that methyl-β-cyclodextrin-pretreated cells failed to open the cytoplasmic domains of the clustered BCR and thus, were unable to transduce signals when recognizing soluble antigens [3]. In contrast, B cells pretreated by DMSO as a control readily formed the typical B cell IS, as examined by TIRFM imaging for the accumulated BCR molecules or by IRM imaging for the tight contact interface (**Fig. 1A**). Statistically, the size of the B cell contact area on antigen-containing PLBs was comparable, as quantified by TIRFM or IRM (Fig. 1A). As TIRFM but not IRM can also evaluate the efficiency of the synaptic accumulation of the molecule of interest by quantifying the fluorescent intensity of the target molecule, we used TIRFM to perform the following imaging experiments.

Next, we tried to identify the molecules that are required for the synaptic recruitment of lipid rafts during B cell activation. In our experimental system, we assessed the accumulation of lipid rafts in B cell IS by use of a lipid raft maker, Lyn-m16-CFP (or Lyn-m16-YFP, termed as Lyn-m16-FP thereafter). Lyn-m16-FP contains the 1st 16 residues of the Src-family kinase Lyn, which leads to the myristoylation and palmitoylation of FP and its tethering to the lipid raft microdomains on the plasma membrane [25, 26]. We asked how the synaptic recruitment of lipid rafts could be affected by cytoskeleton remodeling that is mediated by the dynamic polymerization and de-polymerization of both actin and microtubule molecules. We addressed this question by comparing the quantity of lipid rafts that were accumulated into the B cell IS in DMSO control versus a series of inhibitor-pretreated B cells. Small GTPase, RhoA, and GEF Vav are well-characterized molecules promoting actin polymerization. Here, we found that the RhoA inhibitor (Fig. 1B) and activator (Fig. 1C) significantly impaired the synaptic accumulation of lipid rafts. It is worth noting that the RhoA activator also dramatically impaired the size of B cell IS, whereas the RhoA inhibitor had only a mild effect (Fig. 1B and C). Likewise, the Vav-specific inhibitor 6-Thio-GTP [38]-pretreated B cells showed impaired synaptic accumulation of lipid rafts (Fig. 1D). We continued to evaluate the contribution of microtubule reassembling in the synaptic recruitment of lipid rafts by use of the microtubule polymerization inhibitor nocodazole or de-polymerization inhibitor paclitaxel [21]. Paclitaxel-pretreated CH27 B cells showed a significant impaired synaptic accumulation of lipid rafts (Fig. 1E). Nocodazole-pretreated B cells failed to adhere to the surrogate antigen-containing PLBs (data not shown). It is worth noting that the synaptic accumulations of BCRs in these inhibitor-treated cells were also impaired (Fig. 1B–E), consistent with published studies [20, 21, 44]. Thus, the synaptic recruitment of lipid rafts is a cytoskeleton remodeling-dependent event.

Synaptic recruitment of lipid rafts is regulated by dynein and myosin IIA

We were curious to know if the polarization of lipid rafts to B cell IS is a step facilitated by motor proteins. To check this possibility, we used blebbistatin [33] and HPI-4 [37] inhibitors to block the function of motor proteins myosin IIA and dynein, respectively. Blebbistatin-pretreated CH27 B cells showed a significantly impaired synaptic accumulation of lipid rafts and BCRs (Supplemental Fig. 1A), suggesting that myosin IIA is required

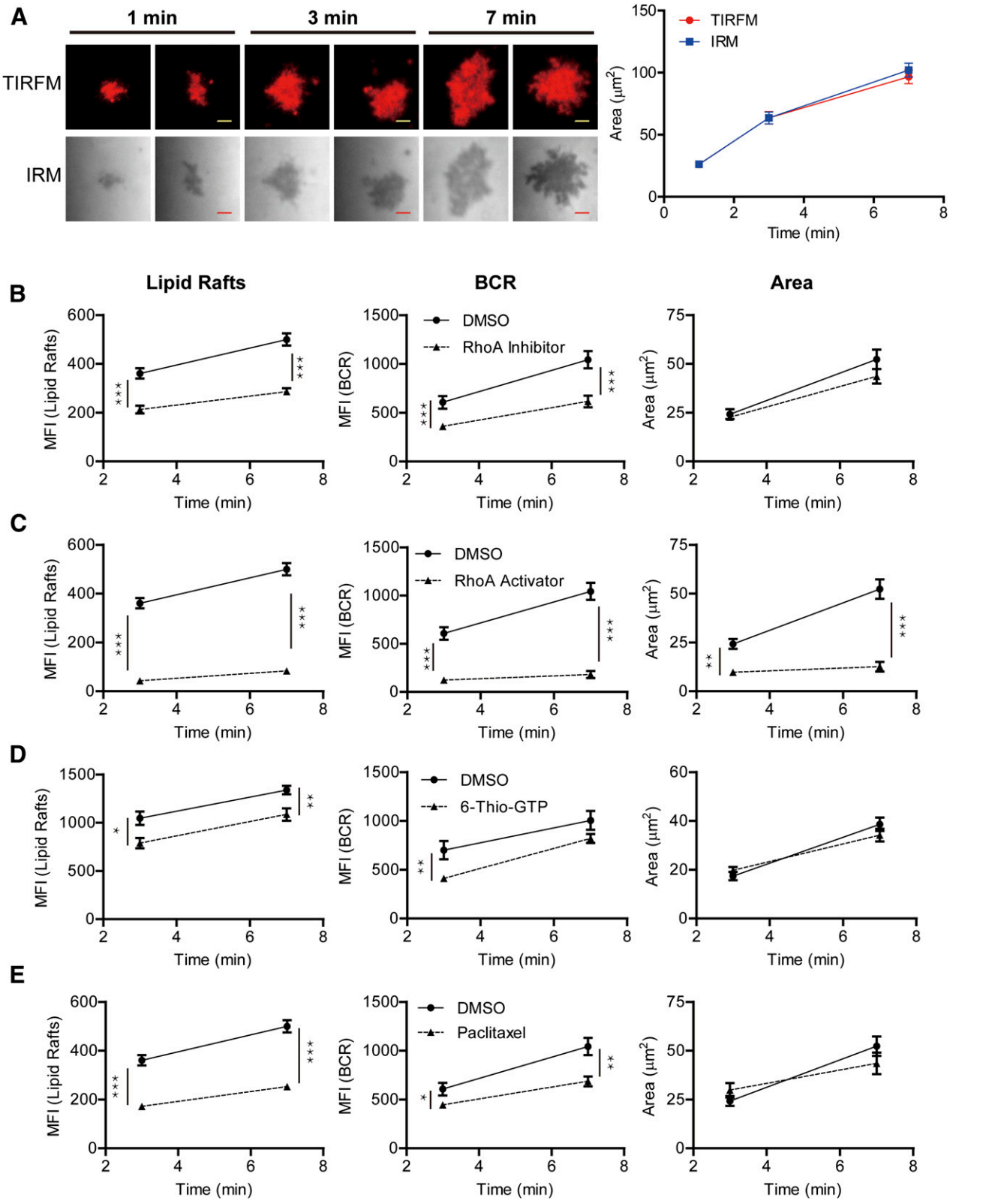

Figure 1. Synaptic recruitment of lipid rafts is dependent on cytoskeleton-remodeling molecules. (A) Comparison of the size of B cell IS by TIRFM or IRM imaging. (Left) Representative images taken by TIRFM or IRM at indicated time points. Scale bars, 3 μm. (Right) Statistical comparison of the size of B cell IS that was quantified by analyzing TIRFM (red) or IRM (blue) images. Shown are means ± SEM of at least 30 cells from 1 representative of 3 independent experiments. (B and C) Small GTPase RhoA inhibitor (B) or RhoA activator (C) was used for the comparison with DMSO control in the

(*continued on next page*)

in this event. However, HPI-4-pretreated CH27 B cells showed a significant enhanced synaptic accumulation of lipid rafts (Supplemental Fig. 1B). We also confirmed this observation in A20II1.6 B cells (Supplemental Fig. 1C). These results from the HPI-4 inhibitor suggest that dynein might promote the clearance of lipid rafts from the B cell IS. Overall, these results show that the synaptic recruitment of lipid rafts is regulated by motor proteins, myosin IIA, and dynein. Myosin IIA promotes the recruitment, whereas dynein promotes the clearance of lipid rafts in the B cell IS. It is worth noting that the synaptic accumulations of BCRs were also likewise affected, as in the case of lipid rafts (Supplemental Fig. 1A–C).

Synaptic recruitment of lipid rafts is triggered by BCR signaling cascades

The mutually correlated phenotype of BCRs and lipid rafts in the inhibitor experiments above suggests that the synaptic recruitment of lipid rafts could be an event that is triggered by BCR signaling molecules. To check this possibility, we used inhibitors against a series of BCR signaling to pretreat the B cells and examined the synaptic accumulation of lipid rafts under each condition compared with DMSO. We first used 2 PI3K inhibitors—wortmannin [30] and LY294002 [31]—to inactivate the function of PI3K, with the consideration that PI3K is an early responding molecule in the cascade of BCR activation regulating the lipid homeostasis of PIP_2 and phosphatidylinositol (3,4,5)-trisphosphate equilibrium. In both cases, we observed significantly impaired accumulation of lipid rafts into the B cell IS in CH27 B cells (**Fig. 2A** and **B**). These observations were also readily repeated in A20II1.6 B cells (Fig. 2C and D). Unsurprisingly, the accumulation of BCRs and the size of B cell IS were also impaired in both cases (Supplemental Fig. 1D–G). These results suggest that PI3K signaling is required for the synaptic recruitment of lipid rafts in B cells.

During B cell activation, PIP_2 is hydrolyzed by the BCR signaling molecule PLCγ2, leading to the production of 2 second messengers: DAG, which is anchored on the inner leaflets of the plasma membrane, and Ca^{2+}, which is freely diffused in the cytosol [4]. Both DAG and Ca^{2+} are second-messenger molecules potently amplifying BCR signal transduction. For DAG, there is a well-characterized equilibrium between DAG and phosphatidic acid that is catalyzed by DGK [45], and DGK inhibitor II pretreated B cells showed dramatically impaired synaptic accumulation of lipid rafts (Fig. 2E), suggesting that the physiologic metabolism of DAG is required for such an event. For Ca^{2+}, we used a Ca^{2+}-chelating agent—BAPTA/AM—to block its normal function [35]. As expected, B cells pretreated with BAPTA/AM also showed decreased efficiency in the recruitment of lipid rafts into the IS (Fig. 2F). Thus, these results suggest that BCR signaling molecules, including second messengers and PI3K, are required for efficient synaptic recruitment of lipid rafts.

Synaptic recruitment of lipid rafts is under strict control of BCR inhibitory coreceptor FcγRIIB and activating coreceptor CD19

The initiation of BCR signaling is known to be regulated by BCR inhibitory coreceptor FcγRIIB and activating coreceptor CD19. In the PI3K and Vav inhibitor results above, it is clear that PI3K and Vav are required for the efficient recruitment of lipid rafts into the B cell IS. As the cytoplasmic tail of CD19 is known for its capability of docking PI3K and Vav signaling molecules [46], thus, we were curious to know the effects of these 2 BCR coreceptors on the synaptic accumulation of lipid rafts. We assessed these effects by comparing the synaptic recruitment of lipid rafts by TIRFM imaging in the condition of BCR cross-linking alone versus the condition of coligating BCR with FcγRIIB or CD19. The experiments showed that FcγRIIB potently inhibits the synaptic accumulation of lipid rafts (Supplemental Fig. 2A). FcγRIIB also inhibited the synaptic recruitment of BCRs (Supplemental Fig. 2B), consistent with our previous studies [29]. The experiments with CD19 showed that coligation of BCR and CD19 dramatically enhanced the synaptic accumulation of both lipid rafts and BCRs compared with the case of BCR cross-linking alone in CH27 B cells (Supplemental Fig. 2C and D) and A20II1.6 B cells (Supplemental Fig. 2E and F). Moreover, we also confirmed that the enhancing function of BCR and CD19 coligation is lipid raft specific. As a control experiment, octadecyl rhodamine B (R18), which is a fluorescent membrane dye that binds to membranes with the fluorophore at the aqueous interface and the alkyl tail, protruding into the lipid interior, did not show such enhanced synaptic accumulation (Supplemental Fig. 2G and H). Overall, these results suggest that the synaptic recruitment of lipid rafts is under the strict control of the BCR inhibitory coreceptor FcγRIIB and activating coreceptor CD19.

Next, we examined the effects of the pharmaceutical inhibitors under the condition of BCR and CD19 coligation. We found that PI3K inhibitors—wortmannin and LY294002—efficiently impaired the accumulation of lipid rafts into the B cell IS compared with the case of DMSO control in the condition of coligating BCR and CD19 (**Fig. 3A** and **B**). Likewise, the blockage of actin remodeling dynamics by small GTPase RhoA inhibitor or activator decreased the synaptic accumulation of lipid rafts under the coligation condition (Fig. 3C). The impaired synaptic accumulation of BCRs was also observed in these experiments (Supplemental Fig. 2I–K). We also observed a similar effect in the synaptic recruitment of lipid rafts in the condition of coligating BCR and CD19 molecules when blocking microtubule depolymerization by paclitaxel (Fig. 3D). Interestingly, motor protein myosin IIA inhibitor blebbistatin decreased (Fig. 3E), whereas dynein inhibitor HPI-4 increased the synaptic accumulation of lipid rafts under the coligation condition (Fig. 3E), consistent with the effects of these 2 motor proteins in the condition of BCR cross-linking alone (Supplemental Fig. 1A–C).

pretreated CH27 B cell. Statistical analyses were given for the synaptic accumulation of lipid rafts (left), BCR (middle), and size of B cell IS (right) at the time points of 3 or 7 min after B cell activation. Shown are means ± SEM of at least 20 cells from 1 representative of 3 independent experiments. (D and E) As in A and B, Vav inhibitor 6-Thio-GTP (D) and microtubule depolymerization inhibitor paclitaxel (E) were used for the comparison with DMSO control. Shown are means ± SEM of at least 18 cells from 1 representative of 3 independent experiments. A Student's *t*-test was performed with the *P* values indicated: $*P < 0.05$, $**P < 0.01$, $***P < 0.001$.

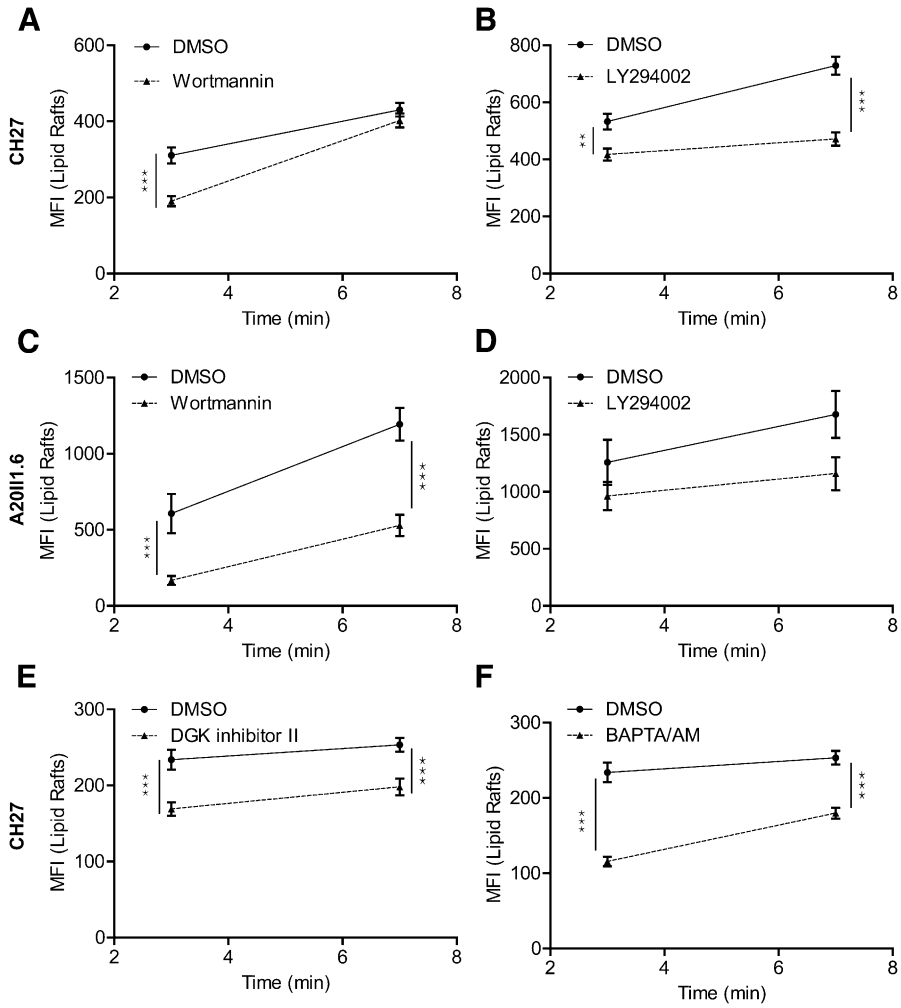

Figure 2. Synaptic recruitment of lipid rafts is triggered by BCR signaling molecules. (A–D) PI3K inhibitors wortmannin (A and C) and LY294002 (B and D) were used for the comparison with DMSO control in pretreated CH27 (A and B) or A20II1.6 B cells (C and D). Statistical analyses were given for the synaptic accumulation of lipid rafts at the time points of 3 or 7 min after B cell activation. Shown are means ± SEM of at least 23 cells from 1 representative of 3 independent experiments. (E and F) As in A and B, DGK inhibitor, DGK inhibitor II (E), or Ca^{2+}-chelating agent, BAPTA/AM (F), were used for the comparison with DMSO control in the pretreated CH27 B cell. Shown are means ± SEM of at least 34 cells from 1 representative of 3 independent experiments. A Student's *t*-test was performed with the *P* values indicated: $^{**}P < 0.01$, $^{***}P < 0.001$.

Lastly, we observed that the DGK inhibitor II and Ca^{2+}-chelating agent BAPTA/AM both significantly impaired the recruitment of lipid rafts into the B cell IS under the coligation condition (Fig. 3F). Over all, these results suggest that the enhanced synaptic recruitment of lipid rafts through the CD19-PI3K module is also under the strict control of actin remodeling and BCR signaling molecules.

Tyr421 and Tyr482 on the cytoplasmic domain of CD19 contribute to the PI3K-dependent accumulation of lipid rafts in the B cell IS

CD19 is known to initiate the activation of a variety of different signaling molecules through its cytoplasmic domain, containing at least 6 key tyrosine residues [47]. We examined which tyrosine residue is responsible for the enhanced lipid raft accumulation by constructing 6 types of CD19 mutates: CD19-Y330F, CD19-Y391F, CD19-Y421F, CD19-Y482F, CD19-Y490F, and CD19-Y513F (**Fig. 4A**). J558L cells lack the expression of endogenous CD19. Thus, we transfected each of these mutant plasmids into J558L cells stably expressing B1-8-High-μ- CFP and Igα-YFP, termed J558L-IgM-B1-8-High, which were established and characterized in our previous studies [21]. Furthermore, the cells were transfected with the Lyn-m16-mCherry plasmid to probe the lipid rafts. J558L-IgM-B1-8-High specifically recognizes hapten antigen NP [48]. Thus, we used PLBs tethering biotin-conjugated NP32-BSA to cross-link BCR alone in J558L-IgM-B1-8-High cells. To compare the effects of CD19-WT and mutants on the synaptic accumulation of lipid rafts, we used PLBs tethering biotin-conjugated NP32-BSA and biotin-conjugated anti-CD19 antibodies to activate these cells under the condition of coligating BCR and CD19 molecules. The results suggested that CD19-WT significantly accumulated 87.3% more lipid raft molecules into the IS under the condition of coligating CD19 and BCR compared with the case of BCR cross-linking alone, consistent with the above-mentioned results in CH27 B cells (Fig. 4B). Four of the CD19 mutants—CD19-Y330F (Fig. 4C), CD19-Y391F (Fig. 4D), CD19-Y490F (Fig. 4E), and CD19-Y513F (Fig. 4F)—showed a similar phenotype as CD19-WT, suggesting that these 4 tyrosines are not essential for the enhanced synaptic accumulation of lipid rafts by CD19 (Fig. 4C–F). However, 2 of these CD19 mutants—CD19-Y421F (Fig. 4G) and CD19-Y482F (Fig. 4H)—lost such enhancing function. Additionally, we used the PI3K inhibitor wortmannin to pretreat J558L-IgM-B1-8-High cells expressing CD19-WT (Fig. 4I) or CD19-Y482F (Fig. 4J) and examined the synaptic accumulation of lipid rafts in the condition of BCR cross-linking alone or in the condition of BCR

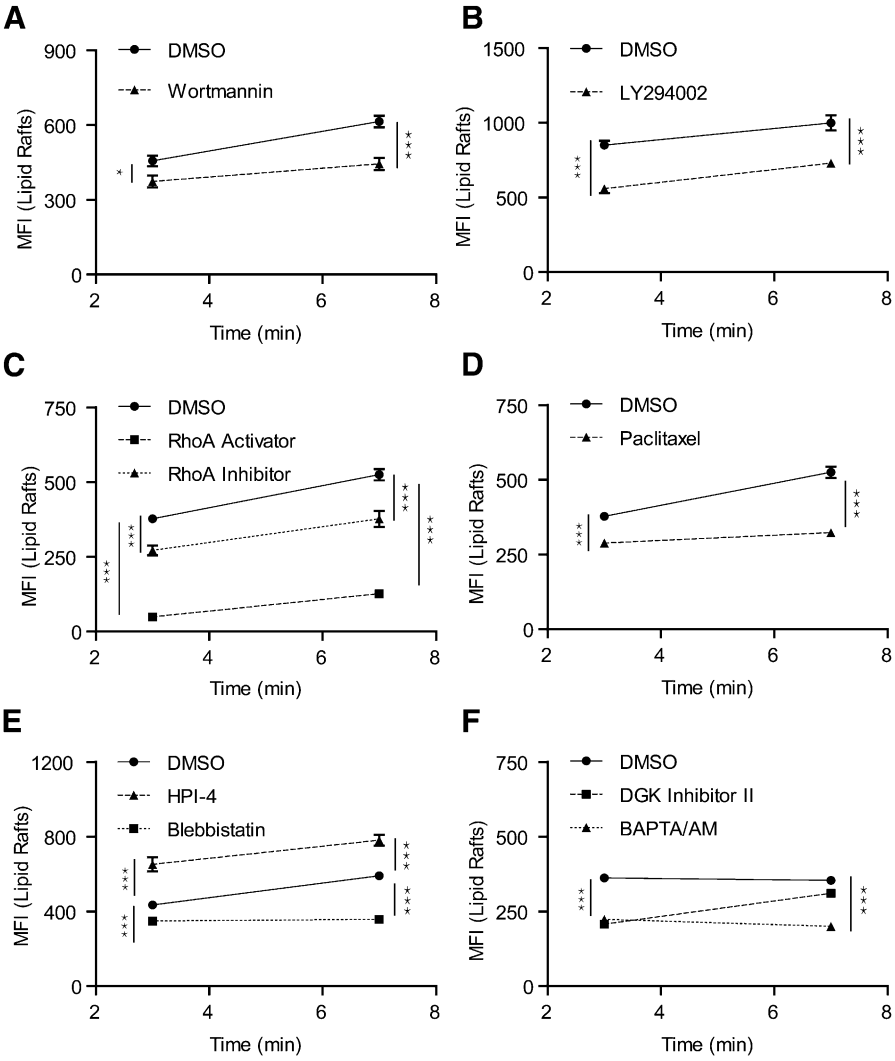

Figure 3. The enhanced synaptic recruitment of lipid rafts through CD19 is under the control of actin remodeling and BCR signaling molecules. (A and B) PI3K inhibitors wortmannin (A) and LY294002 (B) were used for the comparison with DMSO control in the pretreated CH27 B cell in the condition of coligating BCR with CD19. Statistical analyses were given for the synaptic accumulation of lipid rafts at the time points of 3 or 7 min after B cell activation. Shown are means ± SEM of at least 20 cells from 1 representative of 3 independent experiments. (C) Small GTPase RhoA inhibitor or RhoA activator was used for the comparison with DMSO control in the condition of coligating BCR with CD19. Shown are means ± SEM of at least 18 cells from 1 representative of 3 independent experiments. (D and E) Microtubule depolymerization inhibitor paclitaxel (D), motor protein myosin IIA inhibitor blebbistatin (E), and dynein inhibitor HPI-4 (E) were used for the comparison with DMSO control in the condition of coligating BCR with CD19. Shown are means ± SEM of at least 18 cells from 1 representative of 3 independent experiments. (F) DGK inhibitor II and Ca^{2+}-chelating agent BAPTA/AM were used for the comparison with DMSO control in the condition of coligating BCR with CD19. Shown are means ± SEM of at least 42 cells from 1 representative of 3 independent experiments. A Student's *t*-test was performed with the *P* values indicated: $*P < 0.05$, $***P < 0.001$.

and CD19 coligation. B Cells pretreated by wortmannin showed the impaired accumulation of lipid rafts into the B cell IS compared with the case of B cells pretreated by DMSO control under each of these 2 activation conditions (Fig. 4I and J). Moreover, the cells expressing CD19-Y482F did not show significant enhancement after the coligation of BCR and CD19-Y482F in the DMSO control or wortmannin-pretreated condition (Fig. 4J). It is known that phosphorylated Tyr482 provides the major binding site for PI3K in CD19 signaling, whereas phosphorylated Tyr421 is important to recruit Vav and PLCγ2 [47]. Thus, these results further confirmed our conclusion from the above-mentioned pharmaceutical inhibitor studies and emphasized the importance of the CD19-PI3K module in enhancing the synaptic recruitment of lipid rafts in the initiation of B cell activation.

Human peripheral blood primary B cells show enhanced synaptic recruitment of lipid rafts in a PI3K- and cytoskeleton-dependent manner

All of the observations above were acquired from laboratory mouse B cell lines by use of the Lyn-m16-FP marker to quantify the lipid rafts. Next, we used human peripheral blood primary B cells to double check these results. We also used lipid raft marker Alexa Fluor 647-conjugated CTB to label the lipid raft microdomains [49]. We imaged the synaptic recruitment of lipid rafts and BCRs of human primary B cells at 2 time points of 5 and 10 min after loading the cells to PLBs presenting surrogate antigens for BCR cross-linking only or for BCR and CD19 coligation. TIRFM imaging showed that human primary B cells form a typical "bull-eye"-like IS composed of significantly enriched BCR at the center of the contact area of the B cell (or B cell IS; **Fig. 5A**). The significantly enriched BCRs within the center of B cell IS make the quantification of lipid rafts and BCR accumulation by a parameter of MFI inappropriate, as there are very few lipid rafts and BCR molecules within the peripheral area of the B cell IS (Fig. 5A). An analysis simply based on MFI inevitably underestimates the amount of the accumulated lipid rafts within the B cell IS. Thus, instead, we quantified the TFI of both lipid rafts and BCRs in these human primary B cell IS following a reported protocol [20]. The results suggested that CD19-BCR coligation significantly enhanced the synaptic accumulation of lipid rafts (Fig. 5B and C, black, solid line vs. black,

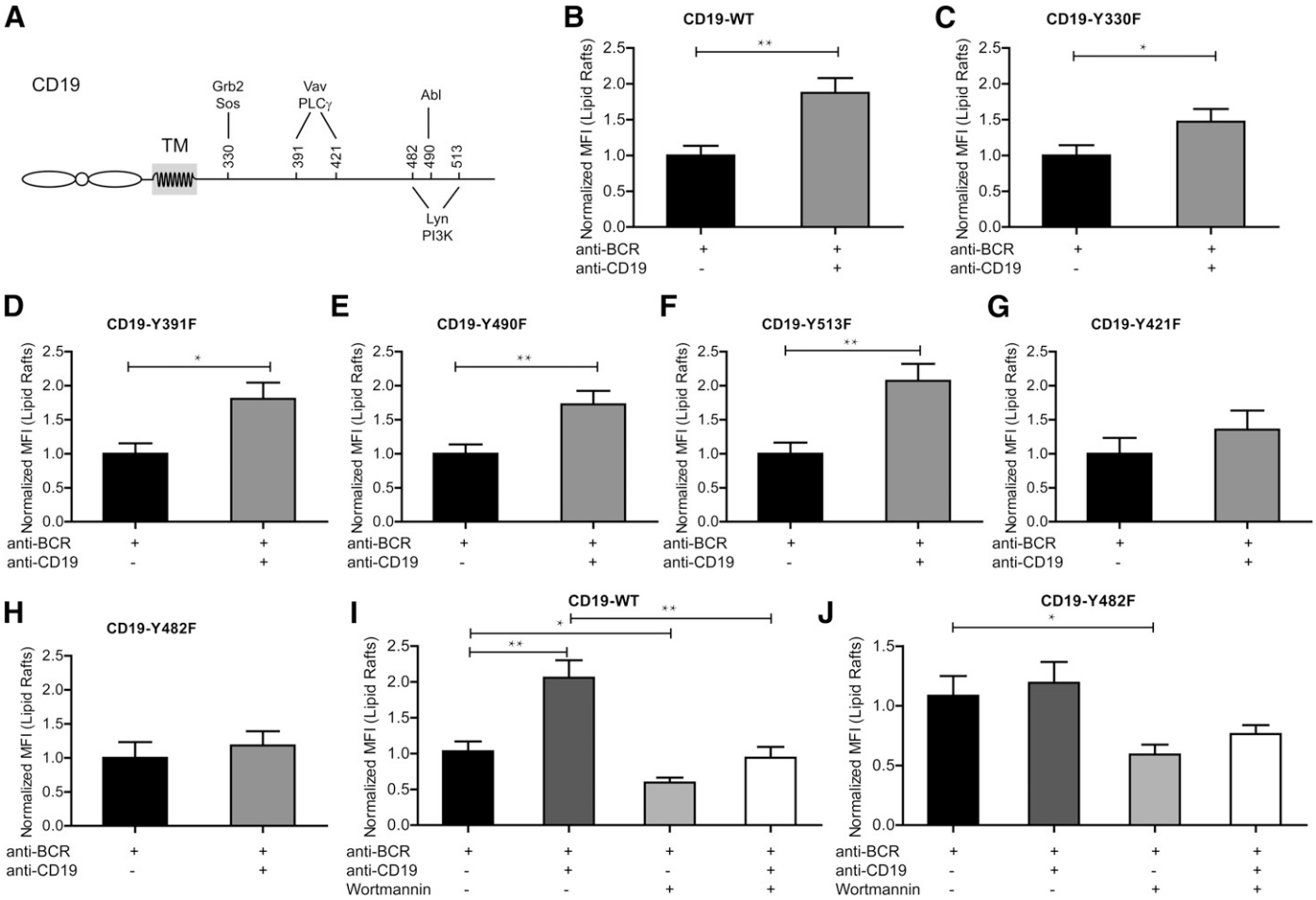

Figure 4. Tyr421 and Tyr482 on the cytoplasmic domain of CD19 contribute to the enhanced accumulation of lipid rafts in the B cell IS. (A) Schematic representation of mouse CD19. The 6 intracellular tyrosine residues are mutated to phenylalanine for a mutagenesis study in this report. These 6 tyrosines are marked with amino acid numbers and the known binding proteins. (B–H) In the condition of BCR cross-linking alone or coligating BCR and CD19-WT (B), CD19-Y330F (C), CD19-Y391F (D), CD19-Y490F (E), CD19-Y513F (F), CD19-Y421F (G), or CD19-Y482F (H), the synaptic recruitment of lipid rafts in J558L cells were, respectively, compared. Shown are means ± SEM of at least 20 cells from 1 representative of 3 independent experiments. (I and J) Wortmannin was used for the comparison with DMSO control in the condition of BCR cross-linking, alone or in the condition of coligating BCR with CD19-WT (I) or CD19-Y482F (J). Shown are means ± SEM of at least 18 cells from 1 representative of 2 independent experiments. A Student's *t*-test was performed with the *P* values indicated: $*P < 0.05$, $**P < 0.01$.

dashed line) and BCRs (Fig. 5D and E). The size of the IS was also increased upon BCR and CD19 coligation (Fig. 5F and G).

The PI3K inhibitor wortmannin dramatically impaired the accumulation of lipid rafts (Fig. 5B) and BCRs into the B cell IS in the condition of BCR cross-linking, alone or in the condition of BCR and CD19 coligation (Fig. 5D, red, solid line vs. red, dashed line). The size of the B cell IS was also decreased dramatically (Fig. 5F). It is worth noting that in human primary B cells pretreated with wortmannin, there is no difference in terms of the synaptic accumulation of lipid rafts and BCRs in the condition of BCR cross-linking alone versus the condition of BCR and CD19 coligation (Fig. 5B and D). Moreover, the effect of the increased size of the B cell IS by CD19 and BCR coligation compared with the condition of BCR cross-linking alone was also blunted in wortmannin-pretreated human primary B cells (Fig. 5F). These results strongly support that the enhanced synaptic recruitment of the lipid rafts and BCRs by CD19 and BCR coligation is a PI3K-dependent event. We also evaluated the effects of the small GTPase RhoA activator in human primary B cells. Consistent with the mouse B cell line data, the RhoA activator significantly impaired the synaptic accumulation of lipid rafts (Fig. 5C) and BCRs (Fig. 5E). The size of the B cell IS was also affected in both cases (Fig. 5G).

Next, we checked the molecular requirement of actin cytoskeleton reassembling in this event by use of actin polymerization inhibitor cytochalasin D [36] and actin depolymerization inhibitor jasplakinolide [21]. Different from mouse CH27 B cells, human primary B cells pretreated by these 2 actin inhibitors maintained their abilities to adhere to the antigen-containing PLBs and form B cell IS, making the evaluation of the contribution of actin remodeling in this event possible (**Fig. 6A**). The results suggested that cytochalasin D (Fig. 6B) and jasplakinolide (Fig. 6C) dramatically impaired the accumulation of lipid rafts and BCRs into the B cell IS in the condition of BCR cross-linking alone or the condition of BCR and CD19 coligation (Fig. 6B and C). Similar to the case of the

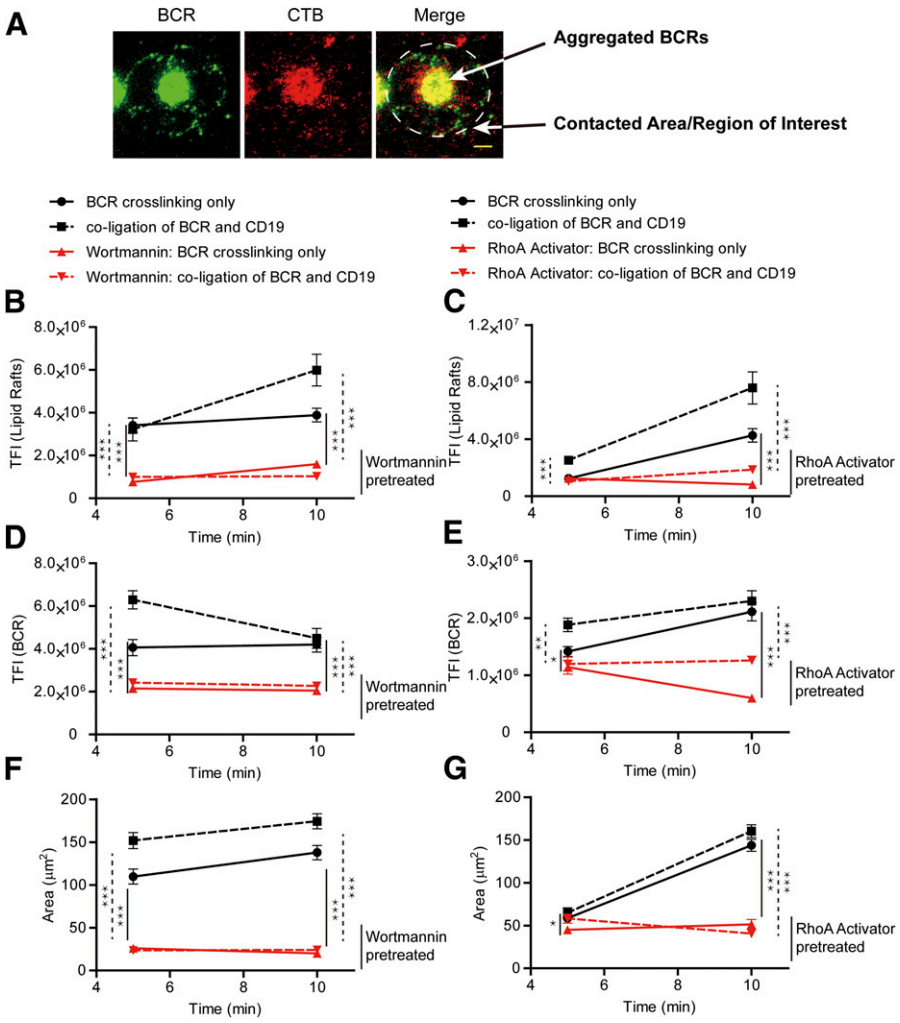

Figure 5. Human peripheral blood primary B cells show enhanced synaptic recruitment of lipid rafts in a CD19-PI3K-dependent manner. (A) Representative TIRFM images of BCR (green) and lipid rafts (red) within the IS of human peripheral blood primary B cells. Scale bar, 1.5 μm. Indicated by arrows are the structure of contacted area/ROI and aggregated BCRs of B cell IS. (B–G) PI3K inhibitors wortmannin (B, D, and F) and small GTPase RhoA activator (C, E, and G) were used for the comparison with DMSO control in human peripheral blood primary B cells at various experimental conditions, as indicated in the figure body. Statistical analyses were given for the synaptic accumulation of lipid rafts (B and C) and BCRs (D and E) and the size (F and G) of the B cell IS at the time points of 5 or 10 min after activating human peripheral blood primary B cells at the condition of BCR cross-linking alone or BCR and CD19 coligation. Shown are means ± SEM of at least 26 cells from 1 representative of 3 independent experiments. A Student's *t*-test was performed with the *P* values indicated: $*P < 0.05$, $**P < 0.01$, $***P < 0.001$.

PI3K inhibitor, actin inhibitors also revoked the enhanced function of CD19 (Fig. 6B and C), suggesting that the enhanced synaptic recruitment of the lipid rafts and BCRs by CD19 and BCR coligation is an actin remodeling-dependent event. Lastly, we used the myosin IIA inhibitor blebbistatin to pretreat the human primary B cells. It is clear that myosin IIA is required for the efficient recruitment of lipid rafts and BCRs into the B cell IS (Fig. 6D), whereas the enhanced effect by CD19 did not seem to require myosin IIA. We also used another myosin IIA inhibitor, ML-7 [39], to confirm these observations (Fig. 6E).

Thus, these experiments in human primary B cells readily confirmed the above-mentioned conclusions from laboratory mouse B cell lines that the synaptic recruitment of lipid rafts is dependent on the CD19-PI3K module and cytoskeleton-remodeling molecules.

DISCUSSION

Lipid rafts function as a central platform in the initiation of B cell activation [5, 6]. Recent advances in high-resolution, high-speed live cell imaging studies suggest that B cell IS is an important membrane-based structure in B cell activation when encountering membrane-bound antigens [14, 15]. By nature, B cell IS is a highly polarized structure composed of synaptically accumulated BCRs, BCR coreceptors, cytoskeleton molecules, motor proteins, second messenger molecules, and signaling transduction molecules. Although B cell IS and lipid rafts are important membrane structures in the initiation of B cell activation, the spatial-temporal distribution of lipid rafts within B cell IS is not clear, nor clear is the refined signaling molecule network supporting the efficient recruitment of lipid rafts into B cell IS.

Sohn et al. [26] systemically investigated the dynamics of the interaction of BCR and lipid raft molecules in B cells encountering membrane-bound antigens. Their study demonstrated that the early-phase association of BCR and lipid raft molecules at the nanometer level is transient, and such transient interaction is independent of BCR signaling molecules and actin cytoskeleton remodeling [26]. However, the association of the BCR and Lyn kinase microcluster is more persistent than the accumulation of BCR microclusters into the B cell IS, and such stable interaction is obviously dependent on Lyn kinase activity [26]. Here, we found that the synaptic recruitment of lipid rafts is dependent on the polymerization, de-polymerization, and repolymerization dynamics of actin and microtubule cytoskeleton, as shown by

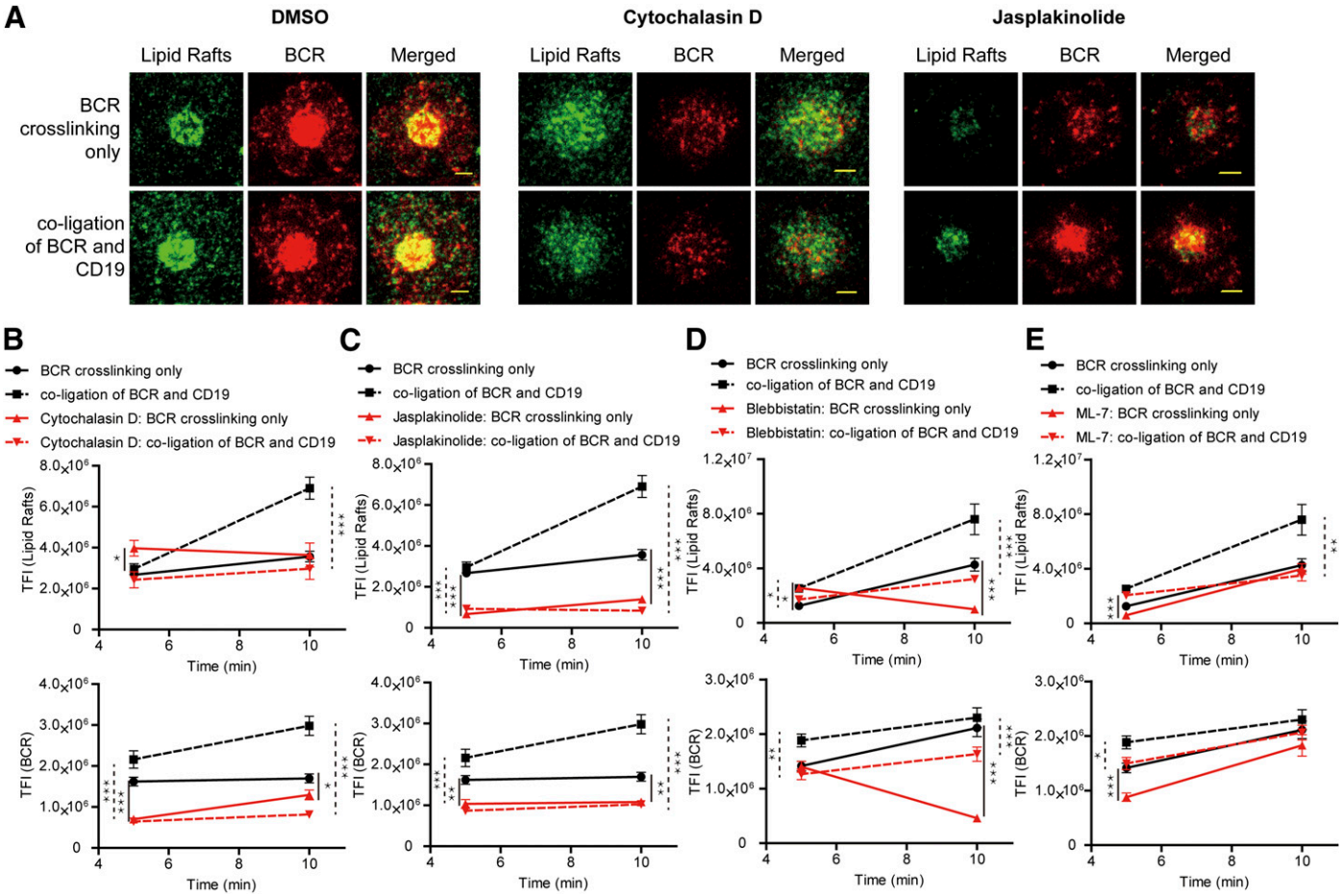

Figure 6. Human peripheral blood primary B cells show enhanced synaptic recruitment of lipid rafts in a cytoskeleton and motor protein-dependent manner. (A) Representative TIRFM images of BCR (red) and lipid rafts (green) within the IS of human peripheral blood primary B cells. Scale bars, 1.5 μm. Given were the representative images from the human peripheral blood primary B cell that were pretreated with DMSO control (left), actin polymerization inhibitor cytochalasin D (middle), or actin de-polymerization inhibitor jasplakinolide (right) at the condition of BCR cross-linking alone (upper) or BCR and CD19 coligation (lower). (B–E) Actin polymerization inhibitor cytochalasin D (B), actin de-polymerization inhibitor jasplakinolide (C), motor protein myosin IIA inhibitor blebbistatin (D), and ML-7 (E) were used for the comparison with DMSO control in human peripheral blood primary B cells at various experimental conditions, as indicated in the figure body. Statistical analyses were given for the synaptic accumulation of lipid rafts (top) and BCRs (bottom) at the time points of 5 or 10 min after activating human peripheral blood primary B cells at the condition of BCR cross-linking alone or BCR and CD19 coligation. Shown are means ± SEM of at least 19 cells from 1 representative of 3 independent experiments. A Student's *t*-test was performed with the *P* values indicated: $*P < 0.05$, $**P < 0.01$, $***P < 0.001$.

TIRFM imaging on pharmaceutical inhibitor-pretreated B cells. As these cytoskeleton remodeling inhibitors also affect the other functions of the cells, such as the shape and adhesion capability [50], we also used small GTPase inhibitors to confirm this conclusion. Small GTPase molecules are well characterized for their key functions in regulating cytoskeleton remodeling [51]. Two small GTPases—RhoA and Rac—are known to link the cross-talk between BCR and actin-remodeling signaling pathway through a common GEF molecule, Vav [52–54]. Indeed, the RhoA activator (or inhibitor) and Rac-specific GEF Vav inhibitor confirmed that the synaptic recruitment of lipid rafts is strictly dependent on cytoskeleton remodeling. These results echo the observations that cytoskeleton-remodeling dynamics is required for the accumulation of BCRs into the B cell IS from our own published studies, as well as those of others [20, 21, 44]. It is not a surprise that the RhoA inhibitor and GEF inhibitors significantly impaired the recruitment of lipid rafts and BCRs into the B cell IS. However, it is truly unexpected that the RhoA activator can also impair such an event and that the reduction of the synaptic recruited lipid rafts and BCRs is even more dramatic than the RhoA inhibitor. All of these results again emphasize that efficient recruitment of lipid rafts and BCRs into the B cell IS requires appropriately balanced actin polymerization and de-polymerization. Our finding here in B cells mirrors the previous studies in T cells showing that lipid raft polarization to the T cell IS is dependent on Vav1, Rac, and actin cytoskeleton re-organization [55]. In their studies, the authors reported that lipid rafts did not translocate to the IS in T cells deficient for Vav1 or in T cells expressing dominant-negative mutants of Vav1 or Rac [55]. Here, it is our new finding that B cells treated with RhoA activator also showed decreased synaptic recruitment of lipid rafts, suggesting that RhoA activation is necessary but not

sufficient to regulate lipid raft polarization at the IS. Our speculation is also supported by the early study that T cells overexpressing Vav1 also failed to induce lipid raft clustering in T cell IS [55].

It is also interesting to observe that the actin-filament motor protein myosin IIA and the microtubule-filament motor protein dynein play opposing roles in this report, with myosin IIA promoting the synaptic recruitment and dynein promoting the synaptic clearance of lipid rafts. These findings on myosin IIA perfectly mirror an early study by Dustin and colleagues [56], showing that the formation and stability of T cell IS are dependent on myosin IIA. Perhaps these results on dynein reflect its function in facilitating the BCR activation-induced internalization or recycling of B cell IS components, including lipid rafts and BCRs. Thus, it is possible that the observation here suggests the delayed clearance of lipid rafts in the IS of B cells with an inactivated dynein motor molecule. Our speculation is supported by a recent study by Schnyder et al. [57], showing that dynein and the microtubule network efficiently promote the centripetal movement of BCR microclusters toward the center of B cell IS. As there is well-documented literature showing that the center area of B cell IS is the major place where B cells internalize BCRs and antigens [58], we propose that a delayed contraction of BCR microclusters into the center of B cell IS will likely decrease the efficiency of clearing lipid rafts from the B cell IS. Thus, it is of genuine interest to investigate the spatial and temporal dynamics of BCRs and lipid rafts during their internalization in B cell IS under the dual regulation of myosin IIA and dynein motor proteins. This speculation is especially interesting with the consideration of the reported studies showing that Myo1C, a single-headed class I myosin, associates with lipid rafts and facilitates their translocation from intracellular compartments to the plasma membrane [59].

Lastly, we showed that the synaptic recruitment of lipid rafts is triggered by a BCR signaling cascades and is under dual regulation of BCR inhibitory coreceptor FcγRIIB and activating coreceptor CD19. These BCR signaling molecules include PI3K, Vav, and 2 major second messengers: Ca^{2+} and DAG. It is worth noting that the function of PI3K and Vav in the synaptic recruitment of lipid rafts is also recapitulated by the results showing the enhancing effects of CD19, as it is known that the cytoplasmic tail of CD19 upon phosphorylation can recruit PI3K and Vav efficiently to the membrane proximal BCR signalosome in B cell activation [47]. The enhanced synaptic recruitment of lipid rafts in a CD19-PI3K-dependent manner is readily confirmed in human primary B cells. Moreover, with the use of the PI3K inhibitor wortmannin, we confirmed that the enhanced synaptic recruitment of the lipid rafts by CD19 and BCR coligation is dependent on PI3K activation. Our findings here provide a mechanistic explanation for the observation in the literature that the coligation of BCR and CD19 increases the amount of BCRs that are translocated into lipid rafts and prolongs their subsequent residency in the lipid rafts [12, 13]. Moreover, the essential function of PI3K in the synaptic accumulation of lipid rafts in activated B cells mirrors the early study that T cells expressing PI3K-dead mutant showed the decreased formation of lipid rafts upon TCR and CD28 coligation [60].

AUTHORSHIP

W.L. and L.X. designed and supervised the experiments. L.X. , A.A., and Y.X. performed the experiments and analyzed the data. F.H. thoroughly edited the manuscript for English content. X.S., Y.L., Z.L., W.Z., and Y-H.C. contributed experimental materials or provided helpful suggestions. W.Z. and Y-H.C. critically revised the article for important intellectual content. W.L. and L.X. wrote the manuscript.

ACKNOWLEDGMENTS

This work is supported by the Ministry of Science and Technology of China (Grants 2014CB542500-03, 2014AA020527), National Science Foundation China (Grants 81361120384, 31270913, 81422020), Beijing Natural Science Foundation (Grant 5132016), Ph.D. Programs Foundation of Ministry of Education of China (Grant 20130002110059), and Tsinghua University Initiative Scientific Research Program (Grant 20131089279). The authors thank Dr. Susan K. Pierce (U.S. National Institutes of Health) for generously providing experimental materials and Zhengpeng Wan and Samina Shaheen (Tsinghua University) for critical comments. L.X. is supported by a postdoctoral fellowship from the Center for Life Sciences of Tsinghua University.

DISCLOSURES

The authors declare no conflict of interest.

REFERENCES

1. Schamel, W. W., Reth, M. (2000) Monomeric and oligomeric complexes of the B cell antigen receptor. *Immunity* **13,** 5–14.
2. DeFranco, A. L. (1993) Structure and function of the B cell antigen receptor. *Annu. Rev. Cell Biol.* **9,** 377–410.
3. Tolar, P., Sohn, H. W., Pierce, S. K. (2005) The initiation of antigen-induced B cell antigen receptor signaling viewed in living cells by fluorescence resonance energy transfer. *Nat. Immunol.* **6,** 1168–1176.
4. Gold, M. R., DeFranco, A. L. (1994) Biochemistry of B lymphocyte activation. *Adv. Immunol.* **55,** 221–295.
5. Dykstra, M., Cherukuri, A., Sohn, H. W., Tzeng, S. J., Pierce, S. K. (2003) Location is everything: lipid rafts and immune cell signaling. *Annu. Rev. Immunol.* **21,** 457–481.
6. Pierce, S. K. (2002) Lipid rafts and B-cell activation. *Nat. Rev. Immunol.* **2,** 96–105.
7. Gupta, N., Wollscheid, B., Watts, J. D., Scheer, B., Aebersold, R., DeFranco, A. L. (2006) Quantitative proteomic analysis of B cell lipid rafts reveals that ezrin regulates antigen receptor-mediated lipid raft dynamics. *Nat. Immunol.* **7,** 625–633.
8. Gupta, N., DeFranco, A. L. (2003) Visualizing lipid raft dynamics and early signaling events during antigen receptor-mediated B-lymphocyte activation. *Mol. Biol. Cell* **14,** 432–444.
9. Gidwani, A., Holowka, D., Baird, B. (2001) Fluorescence anisotropy measurements of lipid order in plasma membranes and lipid rafts from RBL-2H3 mast cells. *Biochemistry* **40,** 12422–12429.
10. Cheng, P. C., Dykstra, M. L., Mitchell, R. N., Pierce, S. K. (1999) A role for lipid rafts in B cell antigen receptor signaling and antigen targeting. *J. Exp. Med.* **190,** 1549–1560.
11. Sohn, H. W., Pierce, S. K., Tzeng, S. J. (2008) Live cell imaging reveals that the inhibitory FcgammaRIIB destabilizes B cell receptor membrane-lipid interactions and blocks immune synapse formation. *J. Immunol.* **180,** 793–799.
12. Cherukuri, A., Cheng, P. C., Pierce, S. K. (2001) The role of the CD19/CD21 complex in B cell processing and presentation of compement-tagged antigens. *J. Immunol.* **167,** 163–172.
13. Cherukuri, A., Cheng, P. C., Sohn, H. W., Pierce, S. K. (2001) The CD19/CD21 complex functions to prolong B cell antigen receptor signaling from lipid rafts. *Immunity* **14,** 169–179.
14. Pierce, S. K., Liu, W. (2010) The tipping points in the initiation of B cell signalling: how small changes make big differences. *Nat. Rev. Immunol.* **10,** 767–777.
15. Harwood, N. E., Batista, F. D. (2010) Early events in B cell activation. *Annu. Rev. Immunol.* **28,** 185–210.

16. Carrasco, Y. R., Batista, F. D. (2007) B Cells acquire particulate antigen in a macrophage-rich area at the boundary between the follicle and the subcapsular sinus of the lymph node. *Immunity* **27,** 160–171.
17. Junt, T., Moseman, E. A., Iannacone, M., Massberg, S., Lang, P. A., Boes, M., Fink, K., Henrickson, S. E., Shayakhmetov, D. M., Di Paolo, N. C., van Rooijen, N., Mempel, T. R., Whelan, S. P., von Andrian, U. H. (2007) Subcapsular sinus macrophages in lymph nodes clear lymph-borne viruses and present them to antiviral B cells. *Nature* **450,** 110–114.
18. Phan, T. G., Grigorova, I., Okada, T., Cyster, J. G. (2007) Subcapsular encounter and complement-dependent transport of immune complexes by lymph node B cells. *Nat. Immunol.* **8,** 992–1000.
19. Qi, H., Egen, J. G., Huang, A. Y., Germain, R. N. (2006) Extrafollicular activation of lymph node B cells by antigen-bearing dendritic cells. *Science* **312,** 1672–1676.
20. Fleire, S. J., Goldman, J. P., Carrasco, Y. R., Weber, M., Bray, D., Batista, F. D. (2006) B Cell ligand discrimination through a spreading and contraction response. *Science* **312,** 738–741.
21. Liu, W., Meckel, T., Tolar, P., Sohn, H. W., Pierce, S. K. (2010) Antigen affinity discrimination is an intrinsic function of the B cell receptor. *J. Exp. Med.* **207,** 1095–1111.
22. Liu, W., Meckel, T., Tolar, P., Sohn, H. W., Pierce, S. K. (2010) Intrinsic properties of immunoglobulin IgG1 isotype-switched B cell receptors promote microclustering and the initiation of signaling. *Immunity* **32,** 778–789.
23. Liu, W., Sohn, H. W., Tolar, P., Pierce, S. K. (2010) It's all about change: the antigen-driven initiation of B-cell receptor signaling. *Cold Spring Harb. Perspect. Biol.* **2,** a002295.
24. Pierce, S. K., Liu, W. (2013) Encoding immunological memory in the initiation of B-cell receptor signaling. *Cold Spring Harb. Symp. Quant. Biol.* **78,** 231–237.
25. Sohn, H. W., Tolar, P., Jin, T., Pierce, S. K. (2006) Fluorescence resonance energy transfer in living cells reveals dynamic membrane changes in the initiation of B cell signaling. *Proc. Natl. Acad. Sci. USA* **103,** 8143–8148.
26. Sohn, H. W., Tolar, P., Pierce, S. K. (2008) Membrane heterogeneities in the formation of B cell receptor-Lyn kinase microclusters and the immune synapse. *J. Cell Biol.* **182,** 367–379.
27. Lakadamyali, M., Rust, M. J., Zhuang, X. (2004) Endocytosis of influenza viruses. *Microbes Infect.* **6,** 929–936.
28. Liu, W., Chen, E., Zhao, X. W., Wan, Z. P., Gao, Y. R., Davey, A., Huang, E., Zhang, L., Crocetti, J., Sandoval, G., Joyce, M. G., Miceli, C., Lukszo, J., Aravind, L., Swat, W., Brzostowski, J., Pierce, S. K. (2012) The scaffolding protein synapse-associated protein 97 is required for enhanced signaling through isotype-switched IgG memory B cell receptors. *Sci. Signal.* **5,** ra54.
29. Liu, W., Won Sohn, H., Tolar, P., Meckel, T., Pierce, S. K. (2010) Antigen-induced oligomerization of the B cell receptor is an early target of Fc gamma RIIB inhibition. *J. Immunol.* **184,** 1977–1989.
30. Ferby, I. M., Waga, I., Hoshino, M., Kume, K., Shimizu, T. (1996) Wortmannin inhibits mitogen-activated protein kinase activation by platelet-activating factor through a mechanism independent of p85/p110-type phosphatidylinositol 3-kinase. *J. Biol. Chem.* **271,** 11684–11688.
31. Vlahos, C. J., Matter, W. F., Hui, K. Y., Brown, R. F. (1994) A specific inhibitor of phosphatidylinositol 3-kinase, 2-(4-morpholinyl)-8-phenyl-4H-1-benzopyran-4-one (LY294002). *J. Biol. Chem.* **269,** 5241–5248.
32. Takesono, A., Heasman, S. J., Wojciak-Stothard, B., Garg, R., Ridley, A. J. (2010) Microtubules regulate migratory polarity through Rho/ROCK signaling in T cells. *PLoS ONE* **5,** e8774.
33. Hung, W. C., Chen, S. H., Paul, C. D., Stroka, K. M., Lo, Y. C., Yang, J. T., Konstantopoulos, K. (2013) Distinct signaling mechanisms regulate migration in unconfined versus confined spaces. *J. Cell Biol.* **202,** 807–824.
34. de Chaffoy de Courcelles, D., Roevens, P., Van Belle, H., Kennis, L., Somers, Y., De Clerck, F. (1989) The role of endogenously formed diacylglycerol in the propagation and termination of platelet activation. A biochemical and functional analysis using the novel diacylglycerol kinase inhibitor, R 59 949. *J. Biol. Chem.* **264,** 3274–3285.
35. Landolfi, B., Curci, S., Debellis, L., Pozzan, T., Hofer, A. M. (1998) Ca2+ homeostasis in the agonist-sensitive internal store: functional interactions between mitochondria and the ER measured In situ in intact cells. *J. Cell Biol.* **142,** 1235–1243.
36. Treanor, B., Depoil, D., Gonzalez-Granja, A., Barral, P., Weber, M., Dushek, O., Bruckbauer, A., Batista, F. D. (2010) The membrane skeleton controls diffusion dynamics and signaling through the B cell receptor. *Immunity* **32,** 187–199.
37. Firestone, A. J., Weinger, J. S., Maldonado, M., Barlan, K., Langston, L. D., O'Donnell, M., Gelfand, V. I., Kapoor, T. M., Chen, J. K. (2012) Small-molecule inhibitors of the AAA+ ATPase motor cytoplasmic dynein. *Nature* **484,** 125–129.
38. Tiede, I., Fritz, G., Strand, S., Poppe, D., Dvorsky, R., Strand, D., Lehr, H. A., Wirtz, S., Becker, C., Atreya, R., Mudter, J., Hildner, K., Bartsch, B., Holtmann, M., Blumberg, R., Walczak, H., Iven, H., Galle, P. R., Ahmadian, M. R., Neurath, M. F. (2003) CD28-dependent Rac1 activation is the molecular target of azathioprine in primary human CD4+ T lymphocytes. *J. Clin. Invest.* **111,** 1133–1145.
39. Barfod, E. T., Moore, A. L., Van de Graaf, B. G., Lidofsky, S. D. (2011) Myosin light chain kinase and Src control membrane dynamics in volume recovery from cell swelling. *Mol. Biol. Cell* **22,** 634–650.
40. Zacharias, D. A., Violin, J. D., Newton, A. C., Tsien, R. Y. (2002) Partitioning of lipid-modified monomeric GFPs into membrane microdomains of live cells. *Science* **296,** 913–916.
41. Gibson, D. G., Young, L., Chuang, R. Y., Venter, J. C., Hutchison III, C. A., Smith, H. O. (2009) Enzymatic assembly of DNA molecules up to several hundred kilobases. *Nat. Methods* **6,** 343–345.
42. Wan, Z., Liu, W. (2012) The growth of B cell receptor microcluster is a universal response of B cells encountering antigens with different motion features. *Protein Cell* **3,** 545–558.
43. Zhang, S., Xu, L., Zhao, X., Chen, X., Fan, Y., Wan, Z., Xu, Y., Liu, W. (2013) A new and robust method of tethering IgG surrogate antigens on lipid bilayer membranes to facilitate the TIRFM based live cell and single molecule imaging experiments. *PLoS ONE* **8,** e63735.
44. Liu, C., Miller, H., Orlowski, G., Hang, H., Upadhyaya, A., Song, W. (2012) Actin reorganization is required for the formation of polarized B cell receptor signalosomes in response to both soluble and membrane-associated antigens. *J. Immunol.* **188,** 3237–3246.
45. Mérida, I., Avila-Flores, A., Merino, E. (2008) Diacylglycerol kinases: at the hub of cell signalling. *Biochem. J.* **409,** 1–18.
46. Depoil, D., Fleire, S., Treanor, B. L., Weber, M., Harwood, N. E., Marchbank, K. L., Tybulewicz, V. L., Batista, F. D. (2008) CD19 is essential for B cell activation by promoting B cell receptor-antigen microcluster formation in response to membrane-bound ligand. *Nat. Immunol.* **9,** 63–72.
47. Mattila, P. K., Feest, C., Depoil, D., Treanor, B., Montaner, B., Otipoby, K. L., Carter, R., Justement, L. B., Bruckbauer, A., Batista, F. D. (2013) The actin and tetraspanin networks organize receptor nanoclusters to regulate B cell receptor-mediated signaling. *Immunity* **38,** 461–474.
48. Sonoda, E., Pewzner-Jung, Y., Schwers, S., Taki, S., Jung, S., Eilat, D., Rajewsky, K. (1997) B Cell development under the condition of allelic inclusion. *Immunity* **6,** 225–233.
49. Floto, R. A., Clatworthy, M. R., Heilbronn, K. R., Rosner, D. R., MacAry, P. A., Rankin, A., Lehner, P. J., Ouwehand, W. H., Allen, J. M., Watkins, N. A., Smith, K. G. (2005) Loss of function of a lupus-associated FcgammaRIIb polymorphism through exclusion from lipid rafts. *Nat. Med.* **11,** 1056–1058.
50. Lin, K. B., Freeman, S. A., Zabetian, S., Brugger, H., Weber, M., Lei, V., Dang-Lawson, M., Tse, K. W., Santamaria, R., Batista, F. D., Gold, M. R. (2008) The rap GTPases regulate B cell morphology, immune-synapse formation, and signaling by particulate B cell receptor ligands. *Immunity* **28,** 75–87.
51. Burridge, K., Wennerberg, K. (2004) Rho and Rac take center stage. *Cell* **116,** 167–179.
52. Saci, A., Carpenter, C. L. (2005) RhoA GTPase regulates B cell receptor signaling. *Mol. Cell* **17,** 205–214.
53. Han, J., Luby-Phelps, K., Das, B., Shu, X., Xia, Y., Mosteller, R. D., Krishna, U. M., Falck, J. R., White, M. A., Broek, D. (1998) Role of substrates and products of PI 3-kinase in regulating activation of Rac-related guanosine triphosphatases by Vav. *Science* **279,** 558–560.
54. Arana, E., Vehlow, A., Harwood, N. E., Vigorito, E., Henderson, R., Turner, M., Tybulewicz, V. L., Batista, F. D. (2008) Activation of the small GTPase Rac2 via the B cell receptor regulates B cell adhesion and immunological-synapse formation. *Immunity* **28,** 88–99.
55. Villalba, M., Bi, K., Rodriguez, F., Tanaka, Y., Schoenberger, S., Altman, A. (2001) Vav1/Rac-dependent actin cytoskeleton reorganization is required for lipid raft clustering in T cells. *J. Cell Biol.* **155,** 331–338.
56. Ilani, T., Vasiliver-Shamis, G., Vardhana, S., Bretscher, A., Dustin, M. L. (2009) T Cell antigen receptor signaling and immunological synapse stability require myosin IIA. *Nat. Immunol.* **10,** 531–539.
57. Schnyder, T., Castello, A., Feest, C., Harwood, N. E., Oellerich, T., Urlaub, H., Engelke, M., Wienands, J., Bruckbauer, A., Batista, F. D. (2011) B Cell receptor-mediated antigen gathering requires ubiquitin ligase Cbl and adaptors Grb2 and Dok-3 to recruit dynein to the signaling microcluster. *Immunity* **34,** 905–918.
58. Lee, S. J., Hori, Y., Chakraborty, A. K. (2003) Low T cell receptor expression and thermal fluctuations contribute to formation of dynamic multifocal synapses in thymocytes. *Proc. Natl. Acad. Sci. USA* **100,** 4383–4388.
59. Brandstaetter, H., Kishi-Itakura, C., Tumbarello, D. A., Manstein, D. J., Buss, F. (2014) Loss of functional MYO1C/myosin 1c, a motor protein involved in lipid raft trafficking, disrupts autophagosome-lysosome fusion. *Autophagy* **10,** 2310–2323.
60. Ladygina, N., Gottipati, S., Ngo, K., Castro, G., Ma, J. Y., Banie, H., Rao, T. S., Fung-Leung, W. P. (2013) PI3Kγ kinase activity is required for optimal T-cell activation and differentiation. *Eur. J. Immunol.* **43,** 3183–3196.

KEY WORDS:
B cell activation · BCR · immunological synapse